Journal of Statistical Physics, Vol. 26, No. 2, 1981

Renormalization Method for Computing the Threshold of the Large-Scale Stochastic Instability in Two Degrees of Freedom Hamiltonian Systems

D. F. Escande[1] and F. Doveil[1]

Received October 28, 1980; revised January 15, 1981

An approximate renormalization procedure is derived for the Hamiltonian $H(v,x,t) = v^2/2 - M\cos x - P\cos k(x-t)$. It gives an estimate of the large scale stochastic instability threshold which agrees within 5–10% with the results obtained from direct numerical integration of the canonical equations. It shows that this instability is related to the destruction of KAM tori between the two resonances and makes the connection with KAM theory. Possible improvements of the method are proposed. The results obtained for H allow us to estimate the threshold for a large class of Hamiltonian systems with two degrees of freedom.

KEY WORDS: Hamiltonian systems; renormalization group; stochasticity; resonance overlap; KAM theory.

1. INTRODUCTION

The transition to the large-scale instability of two-degrees-of-freedom Hamiltonian systems has been a long-standing problem in many fields of physics: astronomy, statistical mechanics, accelerator physics, and plasma physics. The lack of relevant criteria for this transition has been the cause of a large amount of numerical calculations adapted to each specific problem to be solved. The interested reader is referred to four basic proceedings of conferences[1–4] and to the review by Chirikov,[5] which give the principal results and references on the subject.

[1] Laboratoire de Physique des Milieux Ionisés, Ecole Polytechnique, 91128 Palaiseau Cédex, France.

0022-4715/81/1000-0257$03.00/0

Approximate criteria have been derived for this transition (see for instance the review by Lichtenberg in Ref. 4 and the paper by Mo[6]). The most popular among them is the so-called "resonance overlap criterion." Let us first recall the simplest nonintegrable, nonlinear Hamiltonian with two resonant terms,

$$H(v,x,t) = v^2/2 - M\cos x - P\cos k(x-t) \tag{1}$$

which will appear as a paradigm for the two-degrees-of-freedom Hamiltonian systems. In fact H is a time-dependent one-degree-of-freedom Hamiltonian, but it describes the same dynamical system (v,x) as the two-degrees-of-freedom Hamiltonian

$$\mathcal{H}(v,w,x,y) = H(v,x,y) + w \tag{2}$$

as can be seen from the canonical equations. Both H and $\mathcal{H}$ describe the one-dimensional motion of a particle with velocity v in the potential of two longitudinal waves with, respectively, M and P amplitudes, 0 and 1 phase velocities, and k wave number ratio (see Appendix A). We assume in the first two sections that k is a rational number r/p. Therefore $\mathcal{H}$ has periodicity $2p\pi$ in x and y, and the motion takes place on the torus $\{(x,y)$ both in $[-p\pi, p\pi]\}$. The correspondence between H and $\mathcal{H}$ allows us to speak about a motion on a torus even when we deal with H which is explicitly time dependent; t belongs to $\mathbb{R}$. In this section we deal with the phase space $\{(x,v)/x \in [-p\pi, p\pi], v \in \mathbb{R}\}$.

When P is zero we recover the Hamiltonian of the swing (see for instance the study of this Hamiltonian in Ref. 5 and in the paper by Berry in Ref. 2). In this case a resonant domain (where the motion is a libration about the fixed point $x = v = 0$) of half-width $X = 2\sqrt{M}$, centered on $v = 0$, appears in the (v,x) phase space as shown in Fig. 1a. Inside this domain the orbits are said to be trapped by the resonance M. Outside the motion is a rotation and the trajectories in (v,x) are topologically equivalent to the straight lines corresponding to $M = P = 0$.

A similar resonance domain of half-width $Y = 2\sqrt{P}$ exists about $v = 1$ when $M = 0$ and P is nonzero. As this domain moves with a velocity 1, we use a Poincaré map of the system, which is equivalent here to a stroboscopic plot of the system with a period $T = 2\pi/k$. With this map, the resonance domain seems fixed (Fig. 1b). In the following, all the pictures of the phase space are drawn in this manner.

When either M or P is zero, the Hamiltonian (1) is integrable. This is no longer the case when both are nonzero. Physically, when both M and P are small, we can expect that the trajectories between the two resonances are slightly pinched, but conserve their topological nature (Fig. 1c). The phase space picture contains the two unperturbed domains with half-widths

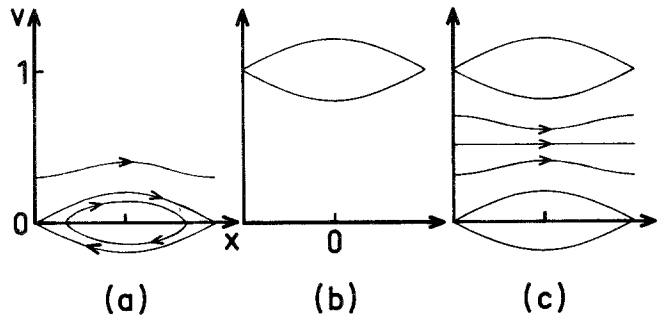

Fig. 1. Sketch of the phase space ($k = 1$). (a) Resonance M alone; (b) resonance P alone; (c) both resonances present.

X and Y and a bunch of slightly perturbed orbits in between. Defining $s = X + Y$, this picture seems likely as long as $s \ll 1$, the unperturbed velocity spacing between the two resonances. When s increases, numerical calculations[1–5] show that the separatrices (the curves which separate the domains of libration and of rotation) burst out into stochastic layers[5] which become larger and larger, and eventually merge between the two resonances. The value s_0 of s where such a merging occurs is called the threshold of the large-scale stochastic instability. For $s \geqslant s_0$, trajectories can diffuse in phase space from the vicinity of the resonance M to that of the resonance P. Chirikov has proposed $s \simeq 1$ as a criterion for this instability.[5] Numerical calculations have shown that this yields the right order of magnitude of s_0 in many cases [more complicated than the case described by the Hamiltonian (1)]. $s = 1$ corresponds to the contact of the unperturbed separatrices of the resonances M and P, so that the criterion $s_0 \simeq 1$ has been called the "resonance overlap criterion."

In fact the resonances do not overlap. This has been shown theoretically[7] and numerically.[8] The physical explanation is the following: let us start with the case $M = P = 0$, and let us consider the orbit associated to $v = 1$ (phase velocity of the resonance P). Then let us increase progressively the value of M from 0. The trace of the $v = 1$ orbit on the Poincaré map will be bent, as it is repelled by the splitting of the $v = 0$ axis into the separatrix of resonance M (Fig. 2a). For a fixed value of M, let us now give a little nonzero value to P. Then the distorted $v = 1$ orbit, will break in its turn into two separatrices having the same shape (Fig. 2b). Indeed the resonance P is repelled by the resonance M. When P increases, it also repells the resonance M, and this gives Fig. 2c. As a consequence, the separatrices which can be computed by a perturbation method[7,8] do not touch for $s = 1$. However, numerical calculations have generally shown that s_0 is smaller than 1. Furthermore, when $M \cdot P \neq 0$, the separatrices do not

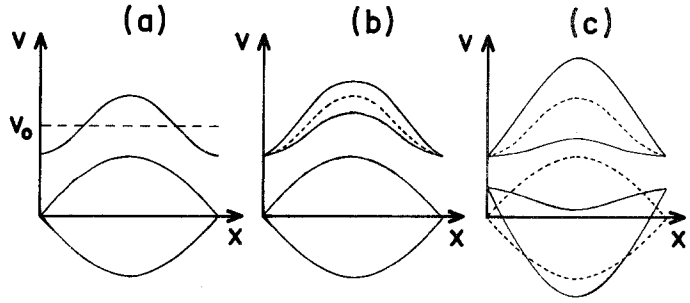

Fig. 2. Repulsion of neighboring resonances. (a) $P = 0$, (b) P small, (c) P and M of the same order of magnitude.

exist any longer and are replaced by thicker and thicker stochastic layers as s increases. The "resonance overlap" is in fact a stochastic layer overlap.

The right understanding of the appearance of stochasticity can only be obtained in the light of the Kolmogorov–Arnold–Moser (KAM) theory.[9] For applying this theory it is more convenient to use the Hamiltonian (2), as it is time independent. Let us write $\mathcal{H} = \mathcal{H}_0(v, w) - V(x, y)$, where $\mathcal{H}_0 = v^2/2 + w$ and $V = M\cos x + P\cos k(x - y)$. The Hamiltonian $\mathcal{H}_0$ is nonlinear and integrable and V is a perturbation. When V is small enough, the KAM theorem states that most of the tori of the $V = 0$ case are preserved. This confirms the physical intuition of Fig. 1. The bent lines in between the resonances M and P on Fig. 1c are the traces of preserved tori on the Poincaré map. The transition to the large-scale stochastic instability corresponds to the destruction of the "last torus" between the resonances M and P (there is probably no last torus since it seems likely that, as long as one torus is preserved, a continuum of tori is preserved in its vicinity).

Greene[10] has studied the standard mapping which corresponds to the Hamiltonian formally defined[5] as

$$K(v, x, t) = v^2/2 - M \sum_{n=-\infty}^{+\infty} \cos(x - nt) \tag{3}$$

which is nothing but the periodization in v of the Hamiltonian H for $M = P$ and $k = 1$. The tori are characterized by their rotation number Q, which is the number of periods T of the stroboscopic flash necessary for x to increase by 2π on the torus. Greene made the assumption that the torus associated to Q is equal to the golden mean was the "last" to disappear. He characterized the destruction of this torus by the destabilization of neighboring periodic orbits. This method gives an estimate of s_0 in good agreement with direct numerical estimates. The trade-off of the method is the necessity to determine the "last" torus (which is not always associated

with the golden mean[11]), and long numerical calculations of the tangent mapping for a whole set of periodic orbits. Furthermore, the method, though efficient, relies upon many unproven assumptions and does not give an explanation of the mechanism of the torus destruction.

In this paper we propose a renormalization method for computing s_0 which also shows how tori are destroyed. Our theory involves some approximations but makes an explicit connection with KAM theory to prove the stability of a given torus. The basic idea of the theory is that of infinitely nested dynamical systems. This idea has been present for a long time in the literature and was made popular by a famous picture of Arnold (Fig. 20.10 of Ref. 9). Ford, quoted by Chirikov in Ref. 5, speaks about Russian dolls. What is new in our theory is that we give the explicit method for going from one system to the next nested one. Figure 3 shows schematically the principle of the renormalization method: the small subsystem in the box between the resonances M and P, becomes through the renormalization transformation a system containing new resonances similar to M and P. As Wilson[12] did, we define a renormalization transformation for the Hamiltonian describing the system.

In Section two we derive the renormalization transformation for Hamiltonians of the type (1). In Section 3 we study this transformation. Section 4 describes the method for computing the threshold, and Section 5 gives possible improvements of the method. Section 6 shows how the previous results can be applied to any two-degrees-of-freedom Hamiltonian system.

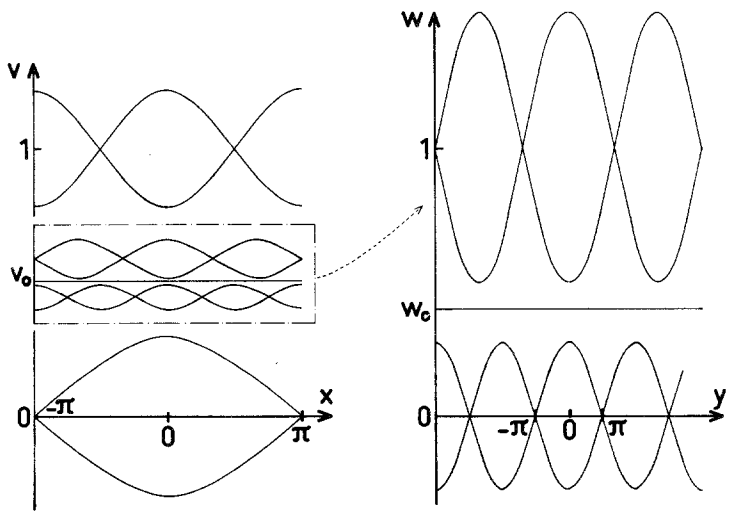

Fig. 3. Graphical description of the renormalization method.

2. DERIVATION OF THE RENORMALIZATION TRANSFORMATION

The dynamical system described by (1) depends on three parameters (M, P, k). Let $\mathcal{T}_0$ be the KAM torus characterized by the rotation number Q_0. We will exhibit an infinite set of nested subdynamical systems which contain this torus. When $M = P = 0$ the velocity on the torus $\mathcal{T}_0$ remains equal to its initial value v_0 along the motion. Q_0 is then given by

$$Q_0 = Q_1(v_0) = 2\pi/(v_0 T) = k/v_0 \tag{4}$$

When $\mathcal{T}_0$ is between the resonances M and P, then $v_0 < 1$ and $Q_0 > k$. When $M \neq 0$ and $P = 0$, H is integrable. We define the action variable for untrapped orbits by

$$I = \frac{1}{2\pi} \int_0^{2\pi} v(x, H_0)\, dx \tag{5}$$

where

$$v(x, H_0) = \left[2(H_0 + M\cos x)\right]^{1/2} \tag{6}$$

It is easy to find

$$I = 4\sqrt{M}\, E(m)/\pi\sqrt{m} \tag{7}$$

with

$$m = 2/(1 + H_0/M) \tag{8}$$

where E is the complete elliptic integral of the second kind.[13] Equations (7) and (8) can be inverted to get H_0 as a function of I, $H_0 = H_0(I)$. The canonical transformation generated by

$$F_A(x, I) = \int^x v\left[z, H_0(I)\right] dz \tag{9}$$

defines the angle variable θ. We now restrict the phase space defined in Section 1 by the conditions $v > 0$ and $m < 1$. This last condition implies that the trajectory is not trapped in the resonance M when $P = 0$, and removes the singularities of the action angle transformation. We get

$$x(I, \theta) = 2am\left[K(m)\theta/\pi, m\right] \tag{10}$$

where m is defined by (8), K is the complete elliptic integral of the first kind, and am is the amplitude.[13] With the above definitions, I tends to v and θ to x, in the limit where M goes to zero. So we expect that for M not too large, the Poincaré map in (v, x) and (I, θ) will be very similar. It is worth noting that the canonical transformation given by F_A appears as a global extension of the Kolmogorov transformation[5] defined by $F_K(x, I) = xI + (M\sin x)/I$ which "kills" the resonance M, since $F_K = F_A + O(\eta^2)$, where $\eta = M/v^2$, without the trouble of a small denominator (see Appendix B).

The equivalent of the velocity is now the transit frequency

$$\Omega(I) = dH_0/dI = \pi\sqrt{M} \Big/ \left[\sqrt{m}\, K(m)\right] \tag{11}$$

For a given M, the action I remains equal on $\mathcal{T}_0$ to its initial value I_0 defined by

$$Q_0 = Q_2(I_0) = 2\pi/(\Omega_0 T) = k/\Omega_0 \tag{12}$$

where $\Omega_0 = \Omega(I_0)$. As $\mathcal{T}_0$ is characterized by the rotation number Q_0, I_0 changes with M according to (12). For $M = 0$, we recover $I_0 = v_0$.

When M and P are both nonzero H becomes, in the previous action angle variables,

$$H'(I,\theta,t) = H_0(I) - P\cos k\left[x(I,\theta) - t\right] \tag{13}$$

As we assumed that k is a rational number r/p, then H' is $2p\pi$ periodic in θ and can be Fourier analyzed:

$$H'(I,\theta,t) = H_0(I) - P\sum_{n=-\infty}^{+\infty} V_n(I)\cos\left[(k+n)\theta - kt\right] \tag{14}$$

This is the first step of the renormalization procedure. The coefficients V_n can be determined analytically only when $2k$ is an integer.[14] As shown in Appendix C, for any k, the V_n's can be expanded in the nome $q(m) = \exp[-\pi K(1-m)/K(m)]$. This yields

$$V_n = \left[2\pi(q/m)^{1/2}/K(m)\right]^{2k}\left[q^n \sum_{l=1}^{n} C_{2k}^{l} C_{n-1}^{l-1} + O(q^{n+2})\right] \tag{15}$$

Where $C_z^l = z(z-1)\cdots(z-l+1)/l!$ for z real and l integer. This is quite a good approximation as long as m is not very close to 1 since q is a very slowly growing function[13] of m. We call resonance R_n, the resonance associated with V_n and lying above $I_s = 4\sqrt{M}/\pi$, the action value at the separatrix of resonance M. As P goes to zero, the phase $(k+n)\theta - kt$ of the resonance R_n is stationary for a value of the action I_n such that $\Omega(I_n) = v_n = k/(k+n)$. According to (12), I_n corresponds to a cycle with a rotation number $Q = k + n$.

H' exhibits an infinity of such resonances. The KAM theorem states that a torus $\mathcal{T}_0$ associated with a sufficiently irrational value of Q_0 is conserved for small enough P. Let n_0 be the integer part of $z = Q_0 - k$. It follows that $v_{n_0} > v_0 > v_{n_0+1}$ and $\mathcal{T}_0$ lies between the resonances R_{n_0} and R_{n_0+1}. In Fig. 4 we have plotted the result of numerical calculations in the case $\rho = X/Y = 1$, $k = 2$, and $s = 0.4$. The Poincaré map is given both in (v,x) space and in (I,θ) space. As expected, as M is not too large, the two plots are very similar above the resonance M. The resonance P corresponds to a chain of two islands, and the resonance R_n to a chain of $2 + n$ islands.

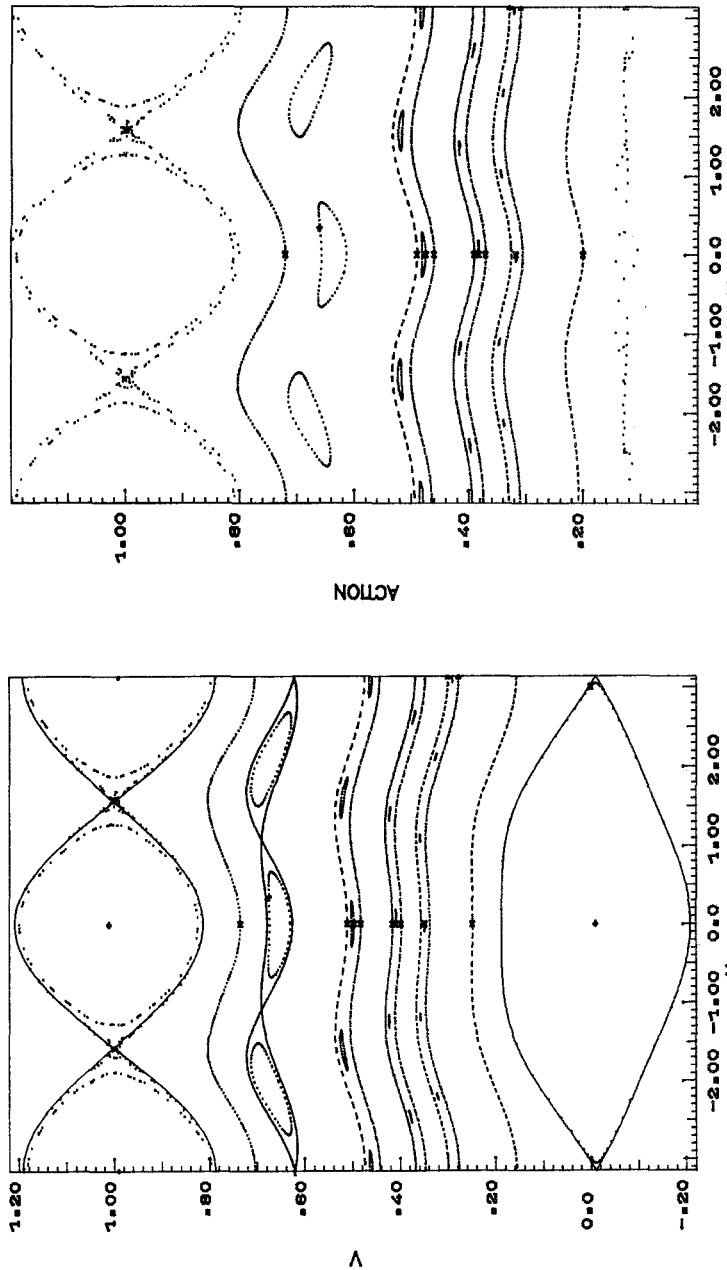

Fig. 4. Poincaré maps of a few trajectories in the (v, x) and (I, θ) planes in the case $k = 2$, $\rho = 1$, $s = 0.4$.

The trapping domain of resonances R_n, $n = 1,2,3,4$, can be seen on the plots. For instance, the n_0 value associated to the torus $\mathcal{T}_0$ corresponding to the untrapped orbit situated between R_1 and R_2, is equal to 1. The continuous lines on the (v,x) plot correspond to a perturbation theory[7,8] prediction of the separatrices of the resonances M, P, and R_1. As the Hamiltonian (1) defined by (M,P,k) and the one defined by $(P,M,1/k)$ correspond to the same dynamical system (cf. Appendix A), when $n_0 = 0$, we replace H by its equivalent

$$H_e(w,y,t') = w^2/2 - P\cos y - M\cos k'(y - t') \tag{16}$$

with $k' = 1/k$. The velocities v and w are related through $v + w = 1$. The rotation number of $\mathcal{T}_0$ in the space (w,y) is given by (4), $Q_0' = k'/w_0 = Q_0/[k(Q_0 - k)]$. It is straightforward to show that $Q_0' > k' + 1$. New v_n's can be computed and it appears that the new n_0 verifies $n_0 \geqslant 1$. Using either H or H_e, we can consider that $n_0 \geqslant 1$ for any $\mathcal{T}_0$ between the resonances M and P.

The second step in the renormalization procedure consists in neglecting all the resonant terms in Eq. (14) except those with $n = n_0$ and $n = n_0 + 1$, which are the most important for determining the stability of $\mathcal{T}_0$: the averaged terms are fast perturbations of the motion with respect to the terms associated to the resonances R_{n_0} and R_{n_0+1}. We then recover a Hamiltonian H'' with two resonances

$$H''(I,\theta,t) = H_0(I) - P\sum_{n=n_0}^{n_0+1} V_n(I)\cos\big[(k+n)\theta - kt\big] \tag{17}$$

H'' describes the strip of the phase space situated between R_{n_0} and R_{n_0+1}. The broadest of the strips situated between the resonances M and P corresponds to $n_0 = 0$. By replacing H by H_e, this large strip splits into smaller ones. As a consequence the choice $n_0 \geqslant 1$ is done for decreasing more rapidly the width of the subsystem enclosing $\mathcal{T}_0$.

As long as P is small, the action $I(t)$ for a trajectory lying on $\mathcal{T}_0$ remains close to the value I_0. For that reason we choose to approximate $H_0(I)$ by its second-order expansion in the vicinity of I_0 (this preserves the nonlinearity of the Hamiltonian) and to approximate the $V_n(I)$'s by $U_n = V_n(I_0)$. This yields the Hamiltonian

$$H^{(3)}(I,\theta,t) = H_0(I_0) + \Omega_0(I - I_0) + \tfrac{1}{2}\sigma_0(I - I_0)^2 - P\sum_{n=n_0}^{n_0+1} U_n\cos\big[(k+n)\theta - kt\big] \tag{18}$$

where $\sigma_0 = \sigma(I_0)$, and $\sigma = d^2H_0/dI^2$. The third step of the renormalization procedure consists in assuming that $H^{(3)}$ correctly describes the stability of

$\mathcal{T}_0$ even for not too small values of P. This assumption seems likely when $\mathcal{T}_0$ is preserved.

We now define

$$y = [k + n_0 + \lambda]\theta - kt \tag{19}$$

where

$$\delta k = z - n_0 = Q_0 - k - n_0 \tag{20}$$

and $\lambda = 0$ (respectively, 1) for $\delta k < \frac{1}{2}$ (respectively, $\delta k > \frac{1}{2}$). We define the canonical transformation from (I, θ) to (J, y) by the generating function[2]

$$F(I, y, t) = I(y + kt)/[k + n_0 + \lambda(\delta k)] + \mu y + \nu t \tag{21}$$

with

$$\mu = (\Omega_0 k_r - \sigma_0 I_0 k_r - k)/\sigma_0 k_r^2 \tag{22}$$

$$k_r = k + n_0 + \lambda \tag{23}$$

$$\nu = \tfrac{1}{2}\sigma_0 k_r^2 \mu^2 + \mu\sigma_0 I_0 k_r + \tfrac{1}{2}\sigma_0 I_0^2 - \Omega_0 I_0 + \mu k + H_0(I_0) - \Omega_0 k_r \mu \tag{24}$$

The new Hamiltonian resulting from this fourth step is

$$H^{(4)}(J, y, t) = \tfrac{1}{2}\sigma_0 k_r^2 J^2 - PU_{n_0+\lambda}\cos y - PU_{n_0+1-\lambda}\cos k'(y - \gamma t) \tag{25}$$

where

$$k' = (k + n_0 + 1 - \lambda)/k_r \tag{26}$$

and

$$\gamma = (2\lambda - 1)k/(k + n_0 + 1 - \lambda) \tag{27}$$

In the new coordinates $\mathcal{T}_0$ is related to $J_0 = (\Omega_0 k_r - k)/(\sigma_0 k_r^2)$.

We then define a new time by $t' = \gamma t$, and a quantity $w = \sigma_0 k_r^2 J/\gamma$. It is straightforward to show that the evolution of $y(t')$ is described by the Hamiltonian

$$H^{(5)}(w, y, t') = w^2/2 - M'\cos y - P'\cos k'(y - t') \tag{28}$$

where

$$M' = PU_{n_0+\lambda}\sigma_0\beta^2 \tag{29}$$

$$P' = PU_{n_0+1-\lambda}\sigma_0\beta^2 \tag{30}$$

$$\beta = (k + n_0)(k + n_0 + 1)/k \tag{31}$$

[2] The canonical transformations for time-dependent Hamiltonians are defined, for instance, in Chap. VII of Ref. 17.

This is the fifth and last step of the procedure. In the new coordinates $\mathcal{T}_0$ is related to a velocity $w_0 = (\Omega_0 k_r - k)/\gamma$ and therefore, according to Eq. (4), to a rotation number $Q' = k'/w_0 = (2\lambda - 1)k/[k_r(\Omega_0 k_r - k)]$. The definition of λ and Eq. (12) yield[3]

$$Q' = Q_0/(k_r|k_r - Q_0|) \tag{32}$$

Between the resonances M' and P' there is a resonance R_1'. The above definition of λ was chosen such that $\mathcal{T}_0$ is between R_1' and M'. Therefore $Q' > k' + 1$, and the condition $n_0 > 1$ is satisfied for any $\mathcal{T}_0$ with $H^{(5)}$. The equations (12), (26), and (28)–(32) define a renormalization transformation[12] T_r of a part of the dynamical system defined by (1) which contains $\mathcal{T}_0$. In the limit where M goes to zero, it is easy to show that $M' = F(n_0 + \lambda, P, M)$, $P' = F(n_0 + 1 - \lambda, P, M)$, where

$$F(l, P, M) = \beta^2(Q_0/2k)^{2l} \sum_l^k PM^l$$

and $\sum_l^k$ is given by formula (C15) of Appendix C. Previously defined for rational k's, T_r can be extended by continuity to real k's.

3. STUDY OF THE RENORMALIZATION TRANSFORMATION

T_r transforms (Q_0, k, M, P) into (Q', k', M', P'). As we shall see now, this transformation splits into simpler transformations. This makes the study easier.

By calculating $z' = Q' - k' = [1 - \lambda - \delta k]/[\delta k - \lambda]$, n' is the integer part of z' (as $Q' > k' + 1$, then $n' > 1$) and $\delta k' = z' - n'$, we can easily show that $\delta k'$ is a function of δk only. Iterating T_r defines the series $\delta k_i, n_i, \lambda_i = \lambda(\delta k_{i-1})$, $i = 1, 2, \ldots,$ which depend only on the initial value δk_0 of δk. The (n_i, λ_i) constitute a coding of δk_0, equivalent to the one given by the coefficients a_i, $i = 1, 2, \ldots,$ of the development of δk_0 into a continuous fraction

$$\delta k_0 = 1/\left[a_1 + 1/(a_2 + 1/\cdots)\right] \tag{33}$$

Table I gives two algorithms to calculate the a_j's from the (n_i, λ_i)'s and reverse.

The $\delta k \to \delta k'$ mapping has everywhere a slope greater than 4 (Fig. 5). This mapping has a denumerable set of fixed points δk_n^λ characterized by the corresponding value of (n, λ). One finds that $\delta k_n^0 = [(n^2 + 2n + 5)^{1/2} - n - 1]/2$ with a_j's given by $a_j = n + 1$; $\delta k_n^1 = [(n^2 + 4n)^{1/2} - n]/2$ with a_j's given by $a_{2l} = n$, $a_{2l+1} = 1$.

[3] As a consequence of the renormalization, the rotation numbers of the resonances $R_{n+\lambda}$ and $R_{n+1-\lambda}$, which were, respectively, $k + n + \lambda$ and $k + n + 1 \mp \lambda$, have become ∞ and k'. It is therefore natural that the rotation number of $\mathcal{T}_0$ change too.

Table I. Correspondence Between a_j and n_i, λ_i

$(n_i, \lambda_i) \to a_j$		$a_j \to (n_i, \lambda_i)$	
(1) Set $j = 0, i = 1$		(1) Set $j = 1, i = 1$	
(2) Is λ_i equal to 0?		(2) Is a_j equal to 1?	
(3) Yes	No	(3) Yes	No
Add 1 to j $a_j = n_i + 1$	Add 1 to j $a_j = 1$ Add 1 to j $a_j = n_i$	$\lambda_i = 1$ $n_i = a_{j+1}$ Add 2 to j	$\lambda_i = 0$ $n_i = a_j - 1$ Add 1 to j
	(4) Add 1 to i (5) Go to step 2		

Equation (26) shows that k' depends on δk, n, and k. When $Q_0 = Q(n, \lambda, k) = k + n + \delta k_n^\lambda$, then n keeps the same value when T_r is iterated, and there exists a $k \to k'$ mapping (Fig. 6) which has a stable fixed point $k_n^\lambda = \delta k_n^\lambda + 1 - \lambda$.

By Eqs. (29) and (30), M' and P' depend on n, δk, k, M, and P. The condition $Q_0 = Q(n, \lambda, k)$ defines a $(k, M, P) \to (k', M', P')$ mapping. For an easier comparison with previous work, we prefer to consider X and Y, the unperturbed widths of the resonances M and P, and to deal with the equivalent mapping $\mathfrak{M} : (k, X, Y) \to (k', X', Y')$. As shown in Fig. 7, $\mathfrak{M}$ has one nontrivial hyperbolic fixed point $\Pi_s = (k_n^\lambda, X_n^\lambda, Y_n^\lambda)$, the stable manifold $\mathbb{S}_n^\lambda$ of which is of dimension 2 (it contains the thick lines of Fig. 7), and four trivial fixed points: $\Pi_0 = (k_n^\lambda, 0, 0)$, $\Pi_1 = (k_n^\lambda, \infty, \infty)$, $\Pi_2 = (k_n^\lambda, 0, \infty)$, and $\Pi_3 = (k_n^\lambda, \infty, 0)$. The points Π_2 and Π_3 belong to the curve C_k^λ of $\mathbb{S}_n^\lambda$ and are sources. The $X = 0$ and $Y = 0$ planes are asymptotes of $\mathbb{S}_n^\lambda$. $\mathbb{S}_n^\lambda$ separates the regions of attraction of Π_0 and Π_1, which are sinks. In a more pictorial way, we may say that a saddle point (Π_s) separates two holes (Π_0, Π_1) and two peaks (Π_2 and Π_3). If the initial point to be renormalized is not just on the crest line (the stable manifold $\mathbb{S}_n^\lambda$ of Π_s) it falls either on Π_0 or on Π_1 as we iterate T_r.

Let us define the line $\mathfrak{D}(k_0, \rho)$ by $k = k_0$ and $X/Y = \rho$. A point $w = (k, X, Y)$ belongs to $\mathfrak{D}(k, X/Y)$, which intersects $\mathbb{S}_n^\lambda$ at $(k, X_n^\lambda, Y_n^\lambda)$. When the stochasticity parameter $s = X + Y$ verifies $s < s_n^\lambda = X_n^\lambda + Y_n^\lambda$, we say that w is under $\mathbb{S}_n^\lambda$ and above $\mathbb{S}_n^\lambda$ in the opposite case. The series $T_r^l(w)$ of the iterates of w by T_r converges towards Π_0 in the first case, and towards Π_1 in the second case. When $s = s_n^\lambda$, $T_r^l(w)$ converges towards Π_s.

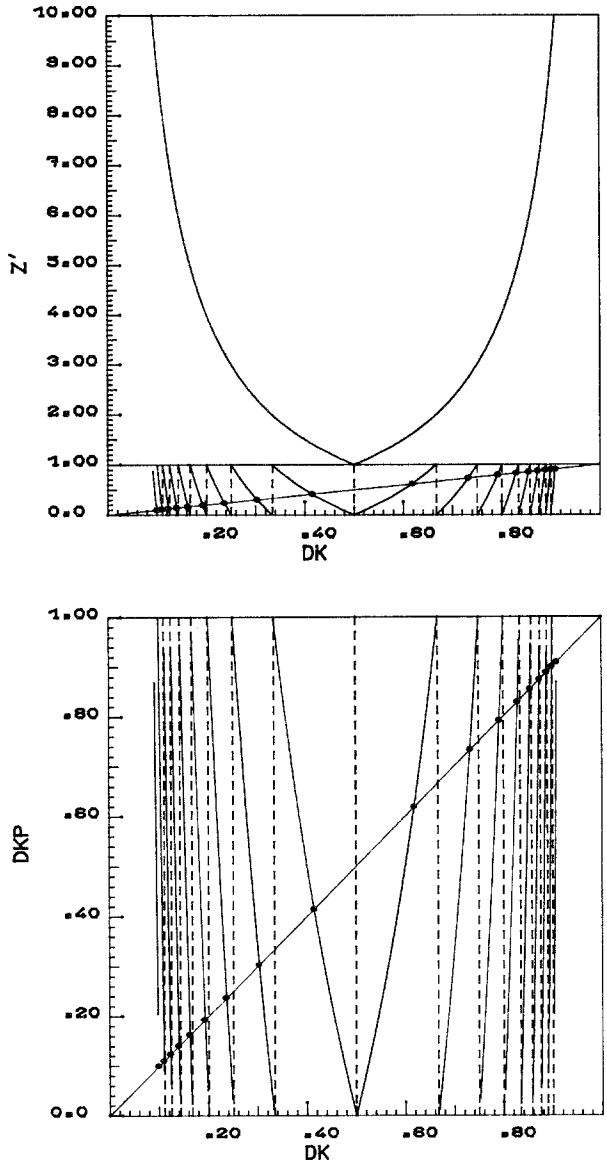

Fig. 5. Plot of $z'(\delta k)$ (upper figure) and $\delta k'(\delta k)$ (lower figure) DKP corresponds to $\delta k'$ and DK to δk.

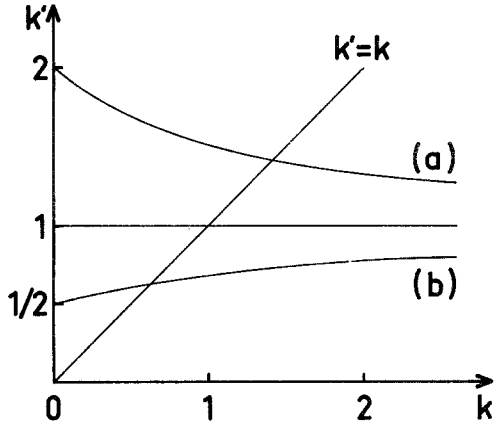

Fig. 6. Plot of $k'(k)$ for $n_0 = 1$ and $\lambda = 0$ (a) and $\lambda = 1$ (b).

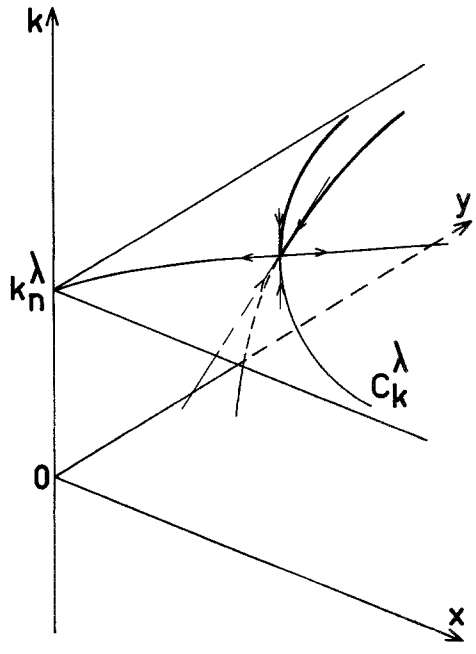

Fig. 7. Hyperbolic fixed point of $\mathfrak{M}$ for (n, λ) fixed.

When w is under $\mathbb{S}_n^\lambda$, for l large enough, $T_r^l(w)$ is in a vicinity of Π_0 where the KAM theorem applies. As a consequence, there exists about $\mathcal{T}_n^\lambda$ ($\mathcal{T}_0$ torus with rotation number Q_n^λ) a continuum of preserved tori and $\mathcal{T}_n^\lambda$ cannot be destroyed, otherwise it would be replaced by a stochastic layer with a finite width which could not be included into a thiner and thiner (as l grows) continuum of tori. So, for w under $\mathbb{S}_n^\lambda$, the original dynamical system contains an infinite series of nested subsystems enclosing a continuum of preserved tori about $\mathcal{T}_n^\lambda$. This continuum is also in the original system, so no trajectory can wander from the stochastic layer of M into the stochastic layer of P. There is no "resonance overlap."

When w is above $\mathbb{S}_n^\lambda$, then $T_r^l(w)$ converges towards Π_1. Unfortunately, at the present time, no mathematical proof of the stochasticity of the system exists. Furthermore, the assumption made in the third step of the procedure that I remains close to I_0 on $\mathcal{T}_0$ becomes questionable. Nevertheless, the results shown at the end of this paper give a strong indication that, in this case, $\mathcal{T}_n^\lambda$ and all the tori in a small vicinity about it are destroyed and have turned into a stochastic layer.

It follows from the above discussion that the present renormalization transformation T_r has a denumerable set of nontrivial (hyperbolic) fixed points [the points of coordinate $(Q_n^\lambda, k_n^\lambda, X_n^\lambda, Y_n^\lambda)$ with $Q_n^\lambda = Q(n, \lambda, k_n^\lambda)$]. The situation is therefore much more intricate than in Wilson's case.[12] Fortunately, we shall show that the knowledge of the $\mathbb{S}_n^\lambda$'s is sufficient to give good estimates to the stochasticity threshold.

4. THRESHOLD OF THE LARGE-SCALE INSTABILITY

It is easy to compute $\mathbb{S}_n^\lambda$ numerically, as it is attractive for any point w iterated through T_r^{-1} with $Q_0 = Q_n^\lambda$. We define the upper envelope of the $\mathbb{S}_n^\lambda$'s as follows: it is, about $X/Y = \rho$ and $k = k_0$, the piece of the surface $\mathbb{S}_{n_0}^{\lambda_0}$ which maximizes the stochasticity parameter s_n^λ.

So far, we only considered tori related to rotation numbers $Q_0 > k + 1$. When $k < Q < k + 1$, we define the surface $\mathbb{S}'$ associated with H_e by the rule that (k, X, Y) belongs to $\mathbb{S}'$ is equivalent to $(1/k, Y, X)$ belongs to $\mathbb{S}$. The upper envelope of $\mathbb{S}$ and $\mathbb{S}'$ is called Σ. For any point w lying under Σ, there certainly exists at least one undestroyed torus $\mathcal{T}_n^\lambda$ for the dynamical system equivalently defined by the Hamiltonians H and H_e. Therefore Σ is under the surface Σ' corresponding to the disappearance of the "last" KAM torus.[4]

[4] Notice that the tori we consider here are those which existed for $s = 0$ and which still exist for a given value of s. For simplicity we call them KAM tori even if the KAM theorem does not apply.

The calculation of Σ' would require consideration of the intricate orbit through T_r of (Q_0, k_0, X_0, Y_0) for any Q_0. This is a difficult and possibly unuseful task since, owing to steps 2 and 3 in Section 2, the renormalization procedure is approximate, and also because we will show later that Σ already gives a good estimation of the true stochasticity threshold Σ_0. In Fig. 8, the section of Σ, for $k = 1$, 2, 3, and 4, is plotted. Recalling that (k, X, Y) and $(1/k, Y, X)$ define the same dynamical system, these curves also give the threshold for $k = \frac{1}{2}$, $\frac{1}{3}$, and $\frac{1}{4}$. The crosses indicate the traces of the intersection of $\mathcal{S}$ and $\mathcal{S}'$, and the dotted line corresponds to Chirikov's criterion.[5] The curves of Fig. 8 are constituted of different pieces of the intersections of $\mathcal{S}_n^\lambda$'s with the plane $k = \text{const}$.

The curve $\rho(v)$ (Fig. 9) yields the value of the velocity v of the "last" torus $(Q = k/v)$ for a given value of ρ for the values $k = 1$, 2, 3, and 4 indicated under each curve. The numbers along the straight vertical lines indicate the value of n corresponding to the torus. When ρ increases, n first decreases, then increases. In the first case the rotation number[5] is $Q = k +$

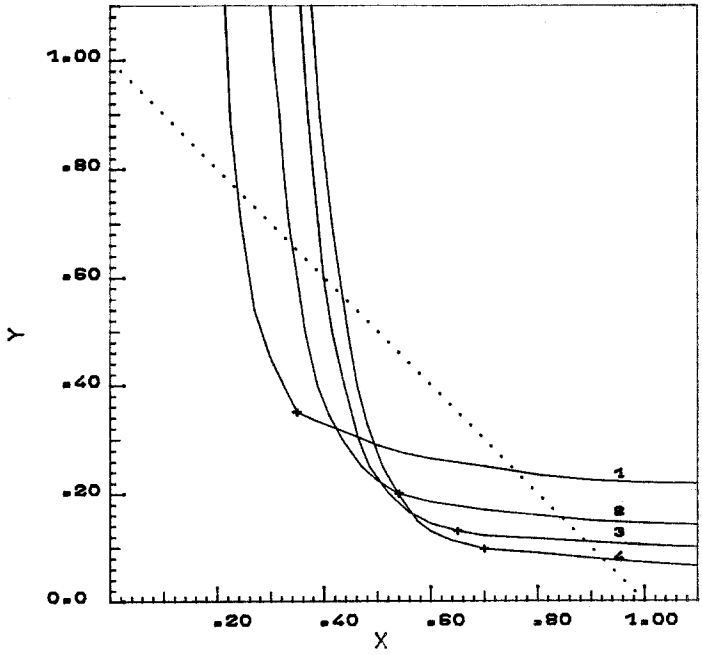

Fig. 8. Sections of surface Σ with $k = \text{const}$ planes. The number on the curve corresponds to the value of k.

[5] Notice that $\lambda = 1$ for every value of n.

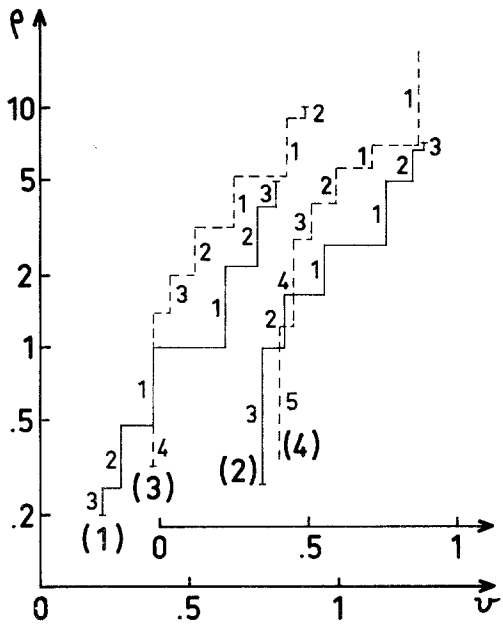

Fig. 9. Velocity v of the "last" torus as a function of ρ for the values $k = 1, 2, 3, 4$ indicated under each curve. The numbers along the straight vertical lines indicate the value of n corresponding to the torus. The v axis is shifted for $k = 2$ and 4. The scale for ρ is logarithmic.

$n + \delta k_n^1$, in the second case $Q = k + 1/(n + \delta k_n^1)$. The v axis is shifted for $k = 2$ and 4. The scale for ρ is logarithmic.

The theoretical threshold can be compared with the one given by numerical integration of the canonical equations for the Hamiltonian (1). Owing to the growth of the correlation time when approaching the stochasticity threshold,[10] we can only compute the value s_τ of s for which a trajectory initiated in the stochastic layer of M makes one turn around the resonance (often called adiabatic) domain of P after a time τ. Therefore s_τ gives an upper bound of the true stochasticity threshold s_0. Numerical results are displayed in Fig. 10 for $\tau = 18{,}400\pi/k$. The solid lines are given by the above presented renormalization theory, the dotted line by the overlap criterion. The values of s_τ are indicated by triangles, the height of which gives the numerical indeterminacy. Figure 10a corresponds to $k = 1$ and $\rho = X/Y$ varying, and Fig. 10b to $\rho = 1$ and k varying. The agreement between the numerical points and the theoretical curve is between 5 and 10%. We shall show in the next section how a better curve (above the present one) can be found for Fig. 10b for $k > 2$.

Owing to the average made in the second step of the renormalization procedure, after each iteration of T_r, we get a dynamical system a little less

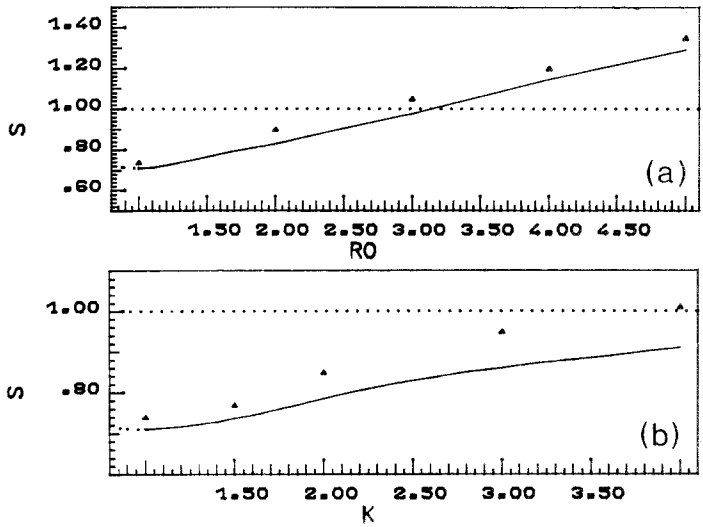

Fig. 10. Stochasticity thresholds for (a) $k = 1$, $X/Y = \mathrm{RO}$ varying (b) $X/Y = 1$, k varying. Continuous lines correspond to the renormalization theory, dotted line to the overlap criterion, and triangles to numerical calculations.

stochastic than the original one. Therefore Σ' is an upper bound to the true stochasticity threshold Σ_0. As Σ is a lower bound to Σ', there remains an indeterminacy for the distance of Σ and the s_τ's from Σ_0. Fortunately, Greene's results[10] allow us to make this point clearer. As told in the Introduction he studied the system described by the Hamiltonian (3). When looking at the resonances with $n = 0$ and $n = 1$, we can define a stochasticity parameter $s = 4\sqrt{M}$. Greene's results correspond to a threshold $s_0 = 0.627$. We have looked at the value of s_τ for the Hamiltonians

$$K_{lm} = v^2/2 - M \sum_{n=l}^{m} \cos(x - nt) \tag{34}$$

for various values of (l, m). The case $(l, m) = (\infty, \infty)$ corresponds to the Hamiltonian (3) and the case $(l, m) = (0, 1)$ to the Hamiltonian (1). When increasing m from 1 and $-l$ from 0, s_τ slightly decreases (the system becomes more stochastic). From this variation, and Greene's value, we can infer the lower bound $s_1 = 0.67$ for s_0 (this calculation also shows that the approximations of step 2 in Section 2 are valid, V_n being a fast decreasing function of n). By direct numerical integration we find that the upper bound of s_0 for $\rho = k = 1$ is $s_2 = 0.74$. The present theory yields $s = 0.6995$, so that the error made on estimating s_0 from Σ is less than 5%. For the case $\rho = k = 1$, Σ corresponds to $\mathbb{S}_1^1$, i.e., to $Q_1^1 = (3 + \sqrt{5})/2$. It can be shown

that only values of Q very close to Q_1^1 can increase the threshold with respect to Σ and that this increase is less than 10^{-3}. For instance the torus with rotation number $Q = 2 + \delta k$, where δk is given by (33) with $a_i = 1$ for $i \neq 3$ and $a_3 = 2$, disappears for $s = 0.6999$. So, Greene's intuition can be stated more precisely: the last KAM tori destroyed are in a small vicinity of the torus associated to the golden mean.

5. POSSIBLE IMPROVEMENTS OF THE METHOD

As mentioned before, a better torus than the $\mathcal{T}_n^\lambda$'s can be found for $k_0 < \frac{1}{2}$ or $k_0 > 2$. Let $\mathbb{S}_{n_0}^{\lambda_0}$ be the part of the upper envelope Σ for the initial values of ρ and k. This surface is related to the torus $\mathcal{T}_{n_0}^{\lambda_0}$ with the rotation number $Q_{n_0}^{\lambda_0}$. For simplicity we assume that ρ remains the same after one iteration of T_r, so that the original point (k_0, X_0, Y_0) and its first iterate through T_r are both in the plane $X = \rho Y$. Figure 11 shows a section of the space (k, X, Y) by this plane; U_ρ corresponds to the direction of the plane. As shown by Eq. (26) and Fig. 6, T_r transforms k_0 into $k'(k_0)$, which belongs to the interval $[\frac{1}{2}, 2]$. Let $\mathbb{S}_{n_1}^{\lambda_1}$ be the part of the upper envelope Σ for $k' = k'(k_0)$ and ρ. The numerical calculations of the preceding section have shown that $\lambda_0 = \lambda_1 = 1$, but that $n_1 \neq n_0$. As shown in Fig. 11, $\mathbb{S}_{n_1}^{\lambda_1}$ is above $\mathbb{S}_{n_0}^{\lambda_0}$ for $k = k'$ and under $\mathbb{S}_{n_0}^{\lambda_0}$ for $k = k_0$ (this results from the definition of the upper envelope). Let us define the torus $\mathcal{T}_0$ related to the rotation number $Q_0 = k_0 + n_0 + \delta k_0$, where $\delta k_0 = [1 + \lambda_1(z' - 1)]/(z' + 1)$ with

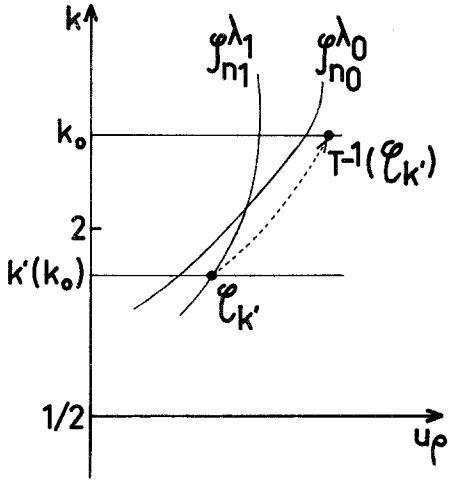

Fig. 11. Graphical proof of the existence of a stabler torus than $\mathcal{T}_{n_0}^{\lambda_0}$.

$z' = n_1 + \delta k_{n_1}^{\lambda_1}$. The image of (Q_0, k_0, X_0, Y_0) by T_r is (Q', k', X', Y'), with $Q' = k' + z'$. From the definition of z' it results that $\delta k' = \delta k_{n_1}^{\lambda_1}$ is a fixed point of the mapping $\delta k \to \delta k'$. Therefore $\mathcal{T}_0$ is stable if (k', X', Y') is under $\mathcal{S}_{n_1}^{\lambda_1}$. The limit of stability of $\mathcal{T}_0$ is the point $T_r^{-1}(\mathcal{C}_{k'})$, where $\mathcal{C}_{k'}$ is the intersection of $\mathcal{S}_{n_1}^{\lambda_1}$ with $k = k'$. Let (k', X', Y') be the coordinates of $\mathcal{C}_{k'}$. From Eqs. (26) and (28)–(32) we can define T_r^{-1} with the here-defined n_0 and $\delta k = \delta k_0$. Let $(Q, k, X, Y) = T_r^{-1}(Q', k', X', Y')$. It results from the definitions of Q_0, k_0, and ρ, that $Q = Q_0$, $k = k_0$, and $\rho = X/Y$. As $\mathcal{C}_{k'}$ is above $\mathcal{S}_{n_0}^{\lambda_0}$, $\lambda_0 = \lambda_1 = 1$ and the definition of Q_0 yields that (k_0, X, Y), denoted in Fig. 11 by $T^{-1}(\mathcal{C}_{k'})$, is above $\mathcal{S}_{n_0}^{\lambda_0}$. $T^{-1}(\mathcal{C}_{k'})$ gives the limit of stability of $\mathcal{T}_0$. As a consequence $\mathcal{T}_0$ disappears later than $\mathcal{T}_{n_0}^{\lambda_0}$ and gives a better estimate of s_0. The corresponding curve is nearer to the numerical points of Fig. 10b.

In the third step of the renormalization procedure, we assumed that $I(t)$ remains close to I_0 on the torus $\mathcal{T}_0$. The (v, x) to (I, θ) transformation has only suppressed the perturbation of the trajectory by the resonance M. In fact the perturbation by the resonance P remains. For that reason, instead of F_A (9), it could be better to use the Kolmogorov transformation from (v, x) to another (I, θ) defined by the generating function

$$F(I, x, t) = Ix + (M \sin x)/I + \left[P \sin k(x - t)\right]/\left[k(I - 1)\right] \quad (35)$$

which "kills" both resonances M and P. It is easily shown that this transformation yields the new Hamiltonian

$$H'(I, \theta, t) = \frac{1}{2} I^2 + \frac{M^2}{4I^2} + \frac{P^2}{4(I-1)^2} + \sum_{n,l} V_{nl}(I) \cos\left[(nk + l)\theta - nkt\right] \quad (36)$$

where the coefficients V_{nl} are exactly computable. Using this transformation, the resonances R_n also appear and a similar renormalization transformation can be defined,[6] which can be interesting for the tori not too near to resonance M or P (I not too close to 0 or 1). With this transformation $I(t)$ is constant up to terms of second order in M or P. This could improve the third step of the procedure.

6. APPLICATION TO TWO-DEGREES-OF-FREEDOM HAMILTONIAN SYSTEMS

Let us consider Hamiltonians of the type

$$H(\mathbf{J}, \boldsymbol{\theta}) = H_0(\mathbf{J}) + \epsilon \sum_{i \in \mathcal{I}} V_i(\mathbf{J}) \cos(\mathbf{p}_i \cdot \boldsymbol{\theta}) \quad (37)$$

[6] The series (36) is double but we retain only the previously defined resonances R_n (related here to V_{n1}), because of the scaling of the V_{nl}'s: if the resonance related to V_{ml} is between R_n and R_{n+1}, then $V_{ml} \ll V_{n+1,1} < V_{n,1}$.

where $\mathbf{J}, \boldsymbol{\theta}, \mathbf{p}_i$ are two-dimensional vectors and $\mathcal{I}$ a set with more than one element. The $\mathbf{p}_i$'s are noncolinear so that H is nonintegrable. Let us define $\omega = \partial H_0/\partial J$. In the limit $\epsilon = 0$, the resonance condition for resonance i is

$$\mathbf{p}_i \cdot \omega(\mathbf{J}) = 0 \tag{38}$$

This defines a value $\mathbf{I}_i$ of $\mathbf{J}$. This value lies on the energy line $H_0(\mathbf{J}) = E$. Therefore the $\mathbf{I}_i$'s are ordered on this line. Let us consider two successive resonances with $i = m$ and $i = p$. Figure 12 shows the plane of the $\mathbf{J}$'s, the energy line, the tangent vectors $\mathbf{m} = \mathbf{p}_m$ and $\mathbf{p} = \mathbf{p}_p$ to this line at $\mathbf{I}_m$ and $\mathbf{I}_p$, and the normal vectors $\omega_i = \omega(\mathbf{I}_i)$. We are interested in the stability of a given torus $\mathcal{T}_0$; it corresponds to the frequency ω_0 which is related in the limit $\epsilon = 0$ to a value $\mathbf{I}_0$ defined by the condition

$$\omega_0 = \omega(\mathbf{I}_0) \tag{39}$$

Let $\mathbf{q}$ be a vector perpendicular to ω_0, and therefore tangent to the energy line at $\mathbf{I}_0$. As done before we forget about the resonant terms other than m and p (when dealing with $\mathcal{T}_0$) by averaging on them. This yields

$$H'(\mathbf{J}, \boldsymbol{\theta}) = H_0(\mathbf{J}) + \epsilon \sum_{i=m,\,p} V_i(\mathbf{J}) \cos(\mathbf{p}_i \cdot \boldsymbol{\theta}) \tag{40}$$

We now perform on H' a series of transformations with the underlying idea that the graph of $H_0(\mathbf{J})$ is locally (generically) a parabola with axis ω_0 and tangent to $\mathbf{q}$. With new coordinates along these axes, H_0 is parabolic, and H' becomes equivalent to a one-degree-of-freedom time-dependent Hamiltonian (cf. the correspondence between H and $\mathcal{H}$ of Section 1). Simple approximations will allow us to use the results on the Hamiltonian (1) for determining the stochasticity threshold of $H'(\mathbf{J}, \boldsymbol{\theta})$.

We define the canonical transformation from $(\mathbf{J}, \boldsymbol{\theta})$ to $(\xi, \eta, \varphi, \psi)$ given by the generating function

$$F(\xi, \eta, \boldsymbol{\theta}) = \boldsymbol{\theta} \cdot (\mathbf{I}_0 + \xi \mathbf{q} + \eta \omega_0) \tag{41}$$

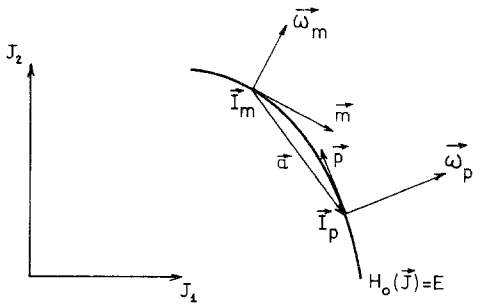

Fig. 12. Energy line $H_0(\mathbf{J}) = E$.

This yields

$$\mathbf{J} = \frac{\partial F}{\partial \boldsymbol{\theta}} = \mathbf{I}_0 + \xi \mathbf{q} + \eta \boldsymbol{\omega}_0 \tag{42}$$

$$\varphi = \frac{\partial F}{\partial \xi} = \mathbf{q} \cdot \boldsymbol{\theta} \tag{43}$$

$$\psi = \frac{\partial F}{\partial \eta} = \boldsymbol{\omega}_0 \cdot \boldsymbol{\theta} \tag{44}$$

Let (α_i, β_i), $i = m, p$, be defined by

$$\mathbf{p}_i = \alpha_i \mathbf{q} - \beta_i \boldsymbol{\omega}_0 \tag{45}$$

Then $\mathbf{p}_i \cdot \boldsymbol{\theta} = \alpha_i \varphi - \beta_i \psi$. Expanding H' in (ξ, η) and retaining the lowest-order terms we get[7]

$$H''(\xi, \eta, \varphi, \psi) = \tfrac{1}{2} a \xi^2 + \omega_0^2 \eta + \epsilon \sum_{i=m,\,p} U_i(\xi, \eta) \cos(\alpha_i \varphi - \beta_i \psi) \tag{46}$$

where $U_i(\xi, \eta) = V_i(\mathbf{J})$, $a = q \sigma_0 q$, $\sigma = \partial \boldsymbol{\omega} / \partial \mathbf{J}$, and $\sigma_0 = \sigma(\mathbf{I}_0)$. The constant term $H_0(\mathbf{I}_0)$ has been omitted as it plays no role in the dynamics. In the limit where $\epsilon = 0$, ξ and η are related through $0 = \frac{1}{2} a \xi^2 + \omega_0^2 \eta$ on the energy line $H_0(\mathbf{I}) = H_0(\mathbf{I}_0)$. This defines $\eta = \eta(\xi)$. As $\eta = O(\xi^2)$ we dropped the terms in $\xi\eta$ and η^2. By using this relation we approximate $U_i(\xi, \eta)$ by $T_i(\xi) = U_i[\xi, \eta(\xi)]$ and we get

$$H^{(3)}(\xi, \eta, \varphi, \psi) = \tfrac{1}{2} a \xi^2 + \omega_0^2 \eta + \epsilon \sum_{i=m,\,p} T_i(\xi) \cos(\alpha_i \varphi - \beta_i \psi) \tag{47}$$

The dynamics of (ξ, φ) defined by (47) are the same as the one defined by

$$H^{(4)}(\xi, \varphi, t) = \tfrac{1}{2} a \xi^2 + \epsilon \sum_{i=m,\,p} T_i(\xi) \cos(\alpha_i \varphi - \gamma_i t) \tag{48}$$

where $\gamma_i = \omega_0^2 \beta_i$.

We now make transformations similar to those of Appendix A. The transformation from (ξ, φ) to (w, x) defined by the generating function

$$F(\xi, x) = \xi(x + \gamma_m t)/\alpha_m + \lambda x + \mu t \tag{49}$$

where $\lambda = -\gamma_m/(a\alpha_m^2)$ and $\mu = a\alpha_m^2 \lambda^2/2 + \gamma_m \lambda$, defines a new Hamiltonian

$$H^{(5)}(w, x, t) = \tfrac{1}{2} a \alpha_m^2 w^2 + \epsilon \{ T_m[\alpha_m(w - \lambda)] \cos x + T_p[\alpha_m(w - \lambda)] \cos(kx - \omega t) \} \tag{50}$$

where $\omega = -\alpha_p(v_m - v_p)$, $v_i = \gamma_i/\alpha_i$, and $k = \alpha_p/\alpha_m$.

[7] As we noticed at the end of Section 2, T_r may be defined for any real value of k. Therefore ω_0 and $\mathbf{q}$ may have real components.

$\mathcal{T}_0$ now corresponds to $w_0 = \lambda$. We define a new time $t' = \omega t/k$, and a new velocity $v = ka\alpha_m^2 w/\omega$. The motion of (v, x) is defined by the Hamiltonian

$$H^{(6)}(v, x, t') = v^2/2 - M(v)\cos x - P(v)\cos k(x - t') \qquad (51)$$

where $M(v)$ and $P(v)$ are $-\epsilon a\alpha_m^2(k^2/\omega^2)T_i[\omega v/(ak\alpha_m) - \alpha_m\lambda]$ for $i = m, p$. This Hamiltonian, apart from the dependence of M and P on v, is the same as (1). $\mathcal{T}_0$ is related to $v_0 = \alpha_p\beta_m/(\alpha_p\beta_m - \alpha_m\beta_p)$.

For each torus we can define a Hamiltonian (51) much simpler than (37), which contains the information about the stability of the torus. In fact if ω_0 and σ_0 do not change too much between $\mathbf{I}_m$ and $\mathbf{I}_p$, the Hamiltonian (51) defined for $\mathbf{I}_0$ colinear to $(\mathbf{I}_m + \mathbf{I}_p)/2$ can describe the stability of all the tori situated between the resonances m and p. Now the ratio $\rho = (M/P)^{1/2}$ is a function of v. A torus $\mathcal{T}_n^\lambda$ is related to a velocity $v_n^\lambda = k/Q_n^\lambda$, and consequently to a value $\rho_n^\lambda = \rho(v_n^\lambda)$. The intersection of the line $\mathcal{D}(k, \rho_n^\lambda)$ with $\mathcal{S}_n^\lambda$ yields the threshold ϵ_n^λ for the destruction of the torus $\mathcal{T}_n^\lambda$. Now the v dependence of ρ does not any longer allow for the build up of an upper envelope. Instead of that we must find the largest $\epsilon_n^\lambda = \epsilon_0$, to get an estimation for the onset of the large-scale instability between the resonances m and p of Hamiltonian (37).

A lower bound of ϵ_0 can be obtained if the curve $\rho(v)$ intersects for some value v_n^λ the curve $\rho(v)$ of Fig. 9. Then the part of $\mathcal{S}_n^\lambda$ of interest for computing ϵ_n^λ is a part of the upper envelope Σ. The value of ϵ_n^λ can be therefore deduced from the curves of Fig. 8, and yields a lower bound to ϵ_0.

In any case the $\mathcal{S}_n^\lambda$'s defined for the Hamiltonian (1) are sufficient to estimate the threshold ϵ_0 for a large class of two-degrees-of-freedom Hamiltonian system.

7. CONCLUSION

This renormalization theory, though nonrigorous, gives a basis to the intuitive feeling of infinitely nested dynamical subsystems. It associates the destruction of the tori to the KAM theory and yields a strong indication that the appearance of the large-scale stochastic instability corresponds to the disappearance of the last tori between two resonances. The low rigorous upper bounds given by the mathematicians for the destruction of the tori, are therefore to be attributed to the use of the Kolmogorov transformation which involves small denominators that are avoided by using the action angle transformation.

From a practical point of view, this theory can give better estimates of the threshold s_0 (or ϵ_0) of the large-scale instability than the usual overlap criterion. It shows that for values of ρ and k not too far from 1, the overlap

criterion yields the right order of magnitude for s_0. Moreover it indicates a possible candidate for being the "last torus" in between two resonances. It is important to know the position of this torus because, just above the threshold, the vicinity of this torus is characterized by the largest correlation time for the stochastic instability.

A forthcoming publication will make the connection between torus destruction and the destabilization of neighboring periodic orbits. For (ρ, k) fixed, let $s(Q_0)$ be the threshold for the destruction of $\mathcal{T}_0$. We shall show that the graph of $s(Q_0)$ is a fractal from which the width of any stochastic layer can be deduced. The analogy of the present renormalization procedure with Wilson's one[12] allows us to expect that there is a characteristic exponent for the correlation times (cf. Ref. 5, Fig. 5.3, p. 313) and the Kolmogorov entropy.

Future efforts are necessary to improve the approximations of the present theory. For instance a better method than the averaging one has to be found. In some cases the Kolmogorov transformation seems to be a good candidate.

ACKNOWLEDGMENTS

The authors thank the attendants of the "Séminaire sur les phénomènes stochastiques," and especially J. Lascoux, F. Ledrappier, A. Mehr, G. Schmidt, and B. Souillard for fruitful discussions. They are indebted to G. Gallavotti for his close study of the first version of the paper and for many useful comments.

APPENDIX A. MOTION OF A PARTICLE IN TWO LONGITUDINAL WAVES

This motion is described by the Hamiltonian

$$H(w,z,t) = \tfrac{1}{2}w^2 - \sum_{i=1}^{2} V_i \cos(k_i z - \omega_i t) \tag{A1}$$

where k_i, ω_i, V_i are the wave numbers, frequencies, and amplitudes of the waves $i = 1$ and 2. We define the canonical transformation from (w,z) to (u,x) by the generating function

$$F(w,x,t) = w(x + \omega_1 t)/k_1 + \lambda x + \mu t \tag{A2}$$

where $\lambda = -\omega_1/k_1^2$ and $\mu = k_1^2\lambda^2/2 + \lambda\omega_1$. It yields the new Hamiltonian

$$H'(v,x,t) = \tfrac{1}{2}k_1^2 u^2 - V_1 \cos x - V_2 \cos(kx - \omega t) \tag{A3}$$

with $k = k_2/k_1$ and $\omega = k_2 \Delta v$, $\Delta v = v_2 - v_1$, where $v_i = \omega_i/k_i$ is the phase velocity of the wave i. This transformation corresponds to the change from

the laboratory frame to the $i = 1$ wave frame. Let us define a new time $t' = \omega t/k$, and a new velocity $v = k_1 u/\Delta v$. The motion of (v, x) is described by

$$H''(v, x, t') = \tfrac{1}{2}v^2 - M\cos x - P\cos k(x - t') \tag{A4}$$

where $M = V_1/\Delta v^2$ and $P = V_2/\Delta v^2$. This Hamiltonian is nothing but (1). Therefore the motion of one particle in two one-dimensional longitudinal waves depends only on three parameters M, P, and k.

APPENDIX B. CONNECTION BETWEEN THE ACTION ANGLE AND KOLMOGOROV TRANSFORMATIONS

We consider the action angle transformation (9) in the limit where $\eta = M/v^2$ goes to zero. In this limit, the parameter m defined by (8) is nothing but $m = 4\eta + O(\eta^2)$. Using the asymptotic expansion[13] of E, we get from (7)

$$I = 2(M/m)^{1/2}\left[1 - m/4 + O(m^2)\right] \tag{B1}$$

The definition of m yields

$$(M/m)^{1/2} = \tfrac{1}{2}v\left[1 + 2\eta\sin^2(x/2) + O(\eta^2)\right] \tag{B2}$$

As a result

$$I = v\left[1 - \eta\cos x + O(\eta^2)\right] = v - (M/v)\cos x + vO(\eta^2) \tag{B3}$$

Or equivalently

$$v = I + (M\cos x)/I + IO(\eta^2) \tag{B4}$$

By using the asymptotic expansion[13] for am, we get from (10)

$$x(I, \theta) = \theta + (M\sin\theta)/v^2 + O(\eta^2) \tag{B5}$$

or equivalently

$$\theta = x - (M\sin x)/I^2 + O(\eta^2) \tag{B6}$$

Formulas (B4) and (B6) are to order η^2 the equations corresponding to the Kolmogorov transformation

$$F_K(x, I) = xI + (M\sin x)/I \tag{B7}$$

This relation between F_A and F_K explains why the Kolmogorov transformation has proven to be a good transformation[7,8] for taking into account the perturbation of resonance M by resonance P (and conversely). This transformation gives the same invariants as the first order of Taylor and Laing's method.[15]

APPENDIX C. DERIVATION OF V_ν FOR ν POSITIVE

Let $\tau = 2p\pi$ be the period of H' (14) in θ. V_ν is given by

$$V_\nu = \frac{1}{\tau}\int_0^\tau \exp\left\{ i\left[2k\,am(K\theta/\pi) - (k+\nu)\theta\right]\right\} d\theta \tag{C1}$$

or

$$V_\nu = \frac{1}{\tau}\int_0^\tau \left[f(\theta)\right]^{2k} \exp\left[-i(k+\nu)\theta\right] d\theta \tag{C2}$$

where $f(\theta) = \exp[iam(K\theta/\pi)]$. This function can be expanded in the nome $q(m) = \exp[-\pi K(1-m)/K(m)]$

$$f(\theta) = A\exp(i\theta/2)(1+X) \tag{C3}$$

with

$$A = 2\pi(q/m)^{1/2}/\left[(1-q^2)K(m)\right] \tag{C4}$$

$$X = \sum_{\substack{n=-\infty \\ n\neq 0}}^{+\infty} a_n \exp(in\theta) \tag{C5}$$

$$a_n = (1-q^2)q^n/(1-q^{4n+2}) \qquad n>0 \tag{C6}$$

$$a_{-n} = -(1-q^2)q^{3n-2}/(1-q^{4n-2}) \qquad n>0 \tag{C7}$$

Let $\mu = 2k$, then

$$\left[f(\theta)\right]^\mu = A^\mu \exp(ik\theta)(1+X)^\mu \tag{C8}$$

$(1+X)^\mu$ is given by

$$(1+X)^\mu = 1 + \sum_{l=1}^{\infty} C_\mu^l X^l \tag{C9}$$

with

$$C_\mu^l = \mu(\mu-1)\cdots(\mu-l+1)/l! \tag{C10}$$

When μ is an integer C_μ^l is a binomial coefficient ($C_\mu^l = 0$ for $l > \mu$). X^l can be written

$$X^l = \sum_{(n_1, n_2, \ldots, n_l)} P\exp(i\sigma\theta) \tag{C11}$$

where

$$P = \prod_{j=1}^{l} a_{n_j} \tag{C12}$$

and

$$\sigma = \sum_{j=1}^{l} n_j \tag{C13}$$

The terms in X^l which contribute to the integral (C2) are those for which $\sigma = \nu$. Let us break σ into the parts σ_+ and σ_- obtained, respectively, with positive and negative n_j's. According to (C6) and (C7), $a_n = O(q^n)$ for $n > 0$ and $a_n = O(q^{3|n|-2})$ for $n < 0$. Therefore the product P is of order $\omega = \sum_{n_j>0} n_j + \sum_{n_j<0}(3|n_j| - 2)$.

If $l \leqslant \nu$, then all the n_j's can be positive and $\omega = \sigma$. The contribution to V_ν is of order q^ν. If $l > \nu$, the order is $q^{\nu+2}$ and we neglect the contribution to V_ν. For $l < \nu$, the contribution of X^l to V_ν is $q^\nu \times$ number of $(n_1, n_2, \ldots, n_l)$'s with $\sigma = \nu$ and $n_j \geqslant 1$. It is easy to show that this number is nothing but $C_{\nu-1}^{l-1}$. As a result

$$V_\nu = \Sigma_\nu^k \left[\frac{2\pi}{K(m)} \left(\frac{q}{m} \right)^{1/2} \right]^{2k} q^\nu \tag{C14}$$

with

$$\Sigma_\nu^k = \sum_{l=1}^{\nu} C_{2k}^l C_{\nu-1}^{l-1} + O(q^{\nu+2}) \tag{C15}$$

When $2k$ is an integer, the V_ν's can be rigorously computed by the residue method described in Ref. 14 and by using the expansion near a pole of the elliptic functions given in Ref. 16. This yields

$$V_\nu = \left[\frac{2\pi}{K(m)} \left(\frac{q}{m} \right)^{1/2} \right]^{2k} \frac{q^\nu}{1 - q^{4(k+\nu)}} \Sigma_\nu^k \tag{C16}$$

with $\Sigma_\nu^{1/2} = 1$, $\Sigma_\nu^1 = 1 + \nu$, $\Sigma_\nu^{3/2} = (3/2 + \nu)^2/2 - (2 - m)(K/2\pi)^2$, $\Sigma_\nu^2 = (2 + \nu)^3/6 - (2 - m)(2 + \nu)(K/\pi)^2/3$. This expression reduces to (C14) when q goes to 0.

REFERENCES

1. G. Casati and J. Ford, eds., *Stochastic Behaviour in Classical and Quantum Hamiltonian Systems* (Springer, Berlin, 1979).
2. S. Jorna, ed., *Topics in Nonlinear Dynamics* (American Institute of Physics, New York, 1978).
3. M. Month and J. C. Herrera, eds., *Nonlinear Dynamics and the Beam–Beam Interaction* (American Institute of Physics, New York, 1978).
4. G. Laval and D. Gresillon, eds. *Intrinsic stochasticity in plasmas* (Editions de Physique, Orsay, 1979).
5. B. V. Chirikov, *Phys. Rep.* **52**:263–379 (1979).
6. K. C. Mo, *Physica (Utrecht)* **57**:445–454 (1972).
7. D. F. Escande, Primary resonances do not overlap, in *Intrinsic stochasticity in plasmas*, G. Laval and D. Gresillon, eds. (Editions de Physique, Orsay, 1979).
8. D. F. Escande and F. Doveil, Charged particle trajectories in the field of two electrostatic waves, in *Proceedings of International Conference on Plasma Physics 1980*, Vol. 1, (Fusion Research Association of Japan, Nagoya, 1980), p. 387.
9. V. I. Arnold and A. Avez, *Ergodic Problems of Classical Mechanics* (Benjamin, New York, 1968).

10. J. M. Greene, *J. Math. Phys.* **20**:1183–1201 (1979).
11. J. M. Greene, KAM Surfaces computed from the Henon–Heiles Hamiltonian, in *Nonlinear Dynamics and the Beam–Beam Interaction*, M. Month and J. C. Herrera, eds. (American Institute of Physics, New York, 1978).
12. K. Wilson, *Rev. Mod. Phys.* **47**:773–840 (1975).
13. L. M. Milne–Thomson, Elliptic integrals, in M. Abramowitz and I. A. Stegun, eds., *Handbook of Mathematical Functions* (Dover, New York, 1972).
14. G. R. Smith and N. R. Pereira, *Phys. Fluids* **21**:2253–2262 (1978).
15. J. B. Taylor and E. W. Laing, *Phys. Rev. Lett.* **35**:1306–1307 (1975).
16. E. T. Whittaker and G. N. Watson, *A Course of Modern Analysis* (Cambridge University Press, Cambridge, England, 1969).
17. L. D. Landau and E. M. Lifshitz, *Mechanics* (Pergamon Press, Oxford, 1960).